Identification of Cardiomyocyte-Fated Progenitors from Human-Induced Pluripotent Stem Cells Marked with CD82

AUTHOR(S):

Takeda, Masafumi; Kanki, Yasuharu; Masumoto, Hidetoshi; Funakoshi, Shunsuke; Hatani, Takeshi; Fukushima, Hiroyuki; Izumi-Taguchi, Akashi; ... Shimamura, Teppei; Yoshida, Yoshinori; Yamashita, Jun K.

CITATION:

Takeda, Masafumi ...[et al]. Identification of Cardiomyocyte-Fated Progenitors from Human-Induced Pluripotent Stem Cells Marked with CD82. Cell Reports 2018, 22(2): 546-556

ISSUE DATE:

2018-01-09

URL:

http://hdl.handle.net/2433/230781

Article

Cell Reports

Identification of Cardiomyocyte-Fated Progenitors from Human-Induced Pluripotent Stem Cells Marked with CD82

Graphical Abstract

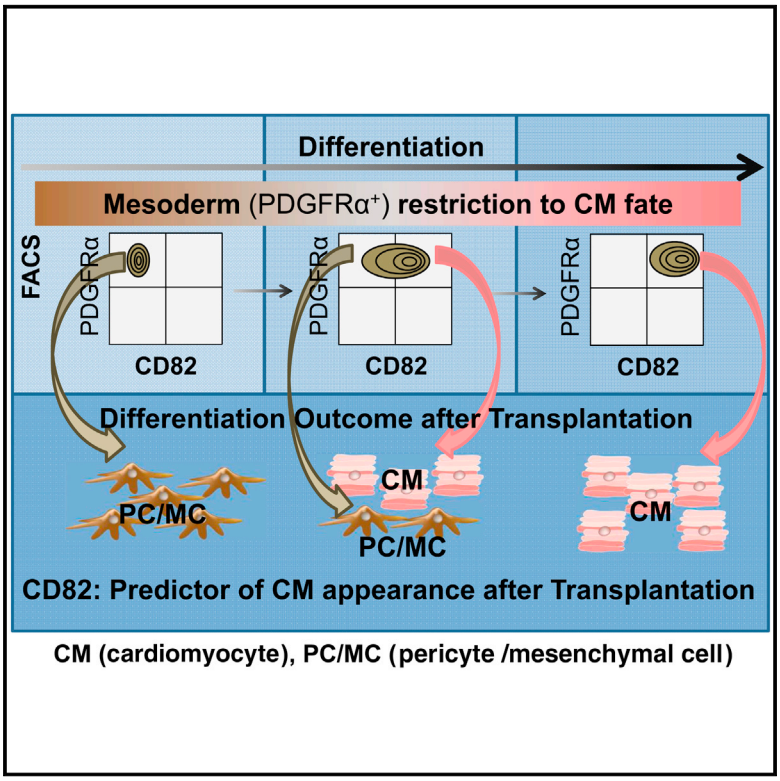

Authors

Masafumi Takeda, Yasuharu Kanki, Hidetoshi Masumoto, ..., Teppei Shimamura, Yoshinori Yoshida, Jun K. Yamashita

Correspondence

juny@cira.kyoto-u.ac.jp

In Brief

Takeda et al. find that CD82^{+} is a cell-surface marker on cardiomyocyte-fated progenitors made from human iPSCs.

Highlights

- Cardiomyocyte (CM)-fated progenitors (CFPs) from human iPSCs
- CD82 as a specific cell-surface CFP marker
- Specific differentiation of CD82^{+} cells to CMs *in vitro* and *in vivo*
- CD82 in CM-fate restriction through exosome-mediated Wnt inhibition

Data and Software Availability

GSE90000
NM_002231

Takeda et al., 2018, Cell Reports *22*, 546–556
January 9, 2018
https://doi.org/10.1016/j.celrep.2017.12.057

CellPress

Cell Reports
Article

Identification of Cardiomyocyte-Fated Progenitors from Human-Induced Pluripotent Stem Cells Marked with CD82

Masafumi Takeda,[1] Yasuharu Kanki,[2] Hidetoshi Masumoto,[1,3] Shunsuke Funakoshi,[4] Takeshi Hatani,[4] Hiroyuki Fukushima,[1] Akashi Izumi-Taguchi,[2] Yusuke Matsui,[5] Teppei Shimamura,[5] Yoshinori Yoshida,[4] and Jun K. Yamashita[1,6,*]

[1]Department of Cell Growth and Differentiation, Center for iPS Cell Research and Application (CiRA), Kyoto University, Kyoto 606-8507, Japan
[2]Isotope Science Center, The University of Tokyo, Tokyo 113-0032, Japan
[3]Department of Cardiovascular Surgery, Kyoto University Graduate School of Medicine, Kyoto 606-8507, Japan
[4]Department of Life Science Frontiers, Center for iPS Cell Research and Application (CiRA), Kyoto University, Kyoto 606-8507, Japan
[5]Division of Systems Biology, Nagoya University Graduate School of Medicine, Nagoya 466-8550, Japan
[6]Lead Contact
*Correspondence: juny@cira.kyoto-u.ac.jp
https://doi.org/10.1016/j.celrep.2017.12.057

SUMMARY

Here, we find that human-induced pluripotent stem cell (hiPSC)-derived cardiomyocyte (CM)-fated progenitors (CFPs) that express a tetraspanin family glycoprotein, CD82, almost exclusively differentiate into CMs both *in vitro* and *in vivo*. CD82 is transiently expressed in late-stage mesoderm cells during hiPSC differentiation. Purified CD82$^+$ cells gave rise to CMs under nonspecific *in vitro* culture conditions with serum, as well as *in vivo* after transplantation to the subrenal space or injured hearts in mice, indicating that CD82 successfully marks CFPs. CD82 overexpression in mesoderm cells as well as in undifferentiated hiPSCs increased the secretion of exosomes containing β-catenin and reduced nuclear β-catenin protein, suggesting that CD82 is involved in fated restriction to CMs through Wnt signaling inhibition. This study may contribute to the understanding of CM differentiation mechanisms and to cardiac regeneration strategies.

INTRODUCTION

Differentiation of pluripotent stem cells (PSCs) to a specific cell type is a process that involves the loss of differentiation potential toward other cell fates. Recent efficient cardiomyocyte (CM) differentiation protocols clarified CM differentiation mechanisms and provided cell types at various differentiation stages (Burridge et al., 2012, 2014). PSCs such as embryonic stem cells (ESCs) and induced PSCs (iPSCs) are induced to the mesoderm, subsequently restricted to cardiac mesoderm composed of cardiovascular progenitor cells (CPCs), and finally committed to CMs. However, there is a missing link during the fate determination process between CPCs and CMs, that is, when and how the CPC fate is restricted to CMs is poorly understood. CPCs that differentiate into CM, endothelial cell (EC), and vascular smooth muscle cell (SMC) lineages have been identified in mice and humans. CPCs have been characterized by the expression of several transcriptional factors, including NK2 homeobox5 (Nkx2.5), Islet1 (Isl1), and mesoderm posterior basic helix-loop-helix transcription factor 1 (Mesp1). In addition, several cell-surface markers have been implicated, including C-X-C chemokine receptor type 4 (CXCR4), receptor tyrosine kinase-like orphan receptor 2 (ROR2), CD13, hyperpolarization-activated cyclic nucleotide-gated channel 4 (HCN4), stage-specific embryonic antigen 1 (SSEA1), glial cell line-derived neurotrophic factor (GDNF) family (GFRA2), kinase insert domain receptor (KDR), and platelet-derived growth factor receptor-α (PDGFRα) (Ardehali et al., 2013; Blin et al., 2010; Burridge et al., 2012; Ishida et al., 2016; Kattman et al., 2011; Moretti et al., 2006; Später et al., 2013; Wu et al., 2006; Yamashita et al., 2000, 2005; Yang et al., 2008). Recently, CPCs were directly reprogrammed from fibroblasts (Lalit et al., 2016; Zhang et al., 2016). CPCs derived from PSCs hold great promise for the study of cardiovascular development as well as for cardiac regeneration. Although CPCs differentiate into CMs with high efficiency in optimized CM differentiation culture conditions *in vitro*, they also show differentiation toward non-CM populations such as vascular or other stromal cell lineages under nonspecific culture conditions or after transplantation *in vivo* (Lalit et al., 2016; Yamashita, 2016). Putative cell populations that exclusively differentiate into CMs even in diverse microenvironments *in vitro* and *in vivo* (here called CM-fated progenitors [CFPs]) are anticipated but remain unknown. Previously, using mouse PSCs, we established a method to systematically induce cardiovascular cells from Flk$^+$ mesoderm cells (Narazaki et al., 2008; Yamashita et al., 2000, 2005). Using human iPSCs (hiPSCs), we reported methods for efficient CM and simultaneous cardiovascular cell differentiation (Masumoto et al., 2014; Uosaki et al., 2011) based on a high-density monolayer culture for human ESCs (Laflamme et al., 2007). In the present study, utilizing our hiPSC differentiation technology, we sought to identify CFPs from hiPSCs.

We defined the timing of CM fate determination during hiPSC differentiation and identified CD82 as a cell-surface marker

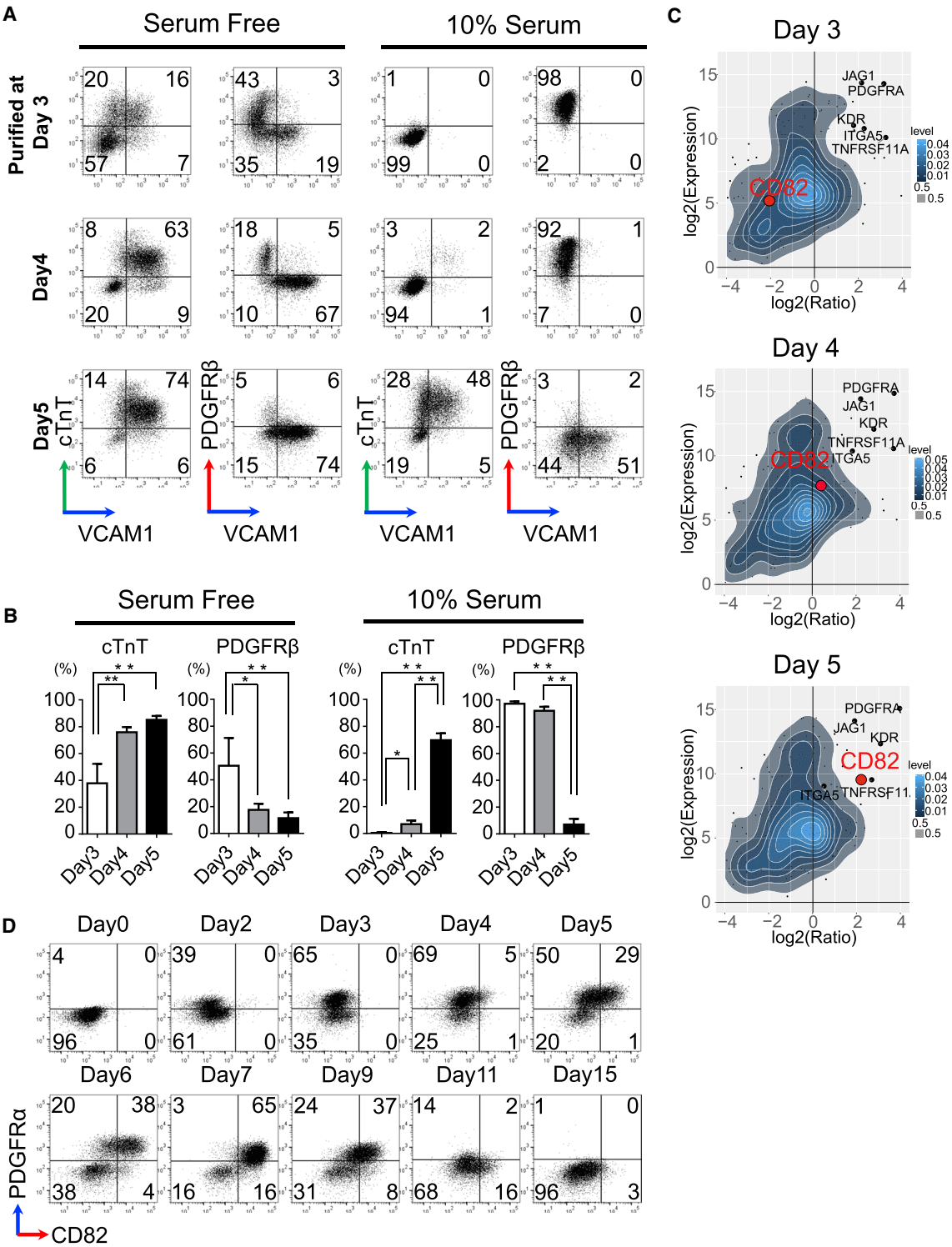

Figure 1. Identification of CD82 as a Candidate Cell-Surface Marker for CFPs

(A) Representative flow cytometric analysis of cTnT, PDGFRβ, and VCAM1. Purified KP-d 3, 4 and 5 were recultured for 14 days in the absence of Wnt inhibitors under serum-free (RPMI1640+B27 supplement) or serum conditions (RPMI1640+10% FBS). Numbers in the quadrants represent the respective percentages of cells.

(B) Quantitative analysis of (A). Data are means ± SDs.

*p < 0.05, **p < 0.01 by one-way ANOVA followed by Tukey's post hoc test (n = 4).

(legend continued on next page)

specifically expressed at the time. CD82 belongs to the tetraspanin family of glycoproteins and was first identified as a metastasis-suppressor gene of prostate cancer (Dong et al., 1995). CD82 is reported to function in cell adhesion, motility and invasion, tumor cell senescence, and exosome production and secretion (Tsai and Weissman, 2011). CD82$^+$ cells overwhelmingly differentiated into CMs *in vitro* and *in vivo*. Moreover, we found a role for CD82 in CM differentiation: Wnt signal inhibition through exosome-mediated β-catenin excretion. Thus, we succeeded in identifying a human CFP population and CM differentiation mechanism.

RESULTS

Identification of CD82 as a Candidate Cell-Surface Marker for CFPs

To identify specific markers of CFPs, we used a previously reported serum-free high-density monolayer culture protocol for hiPSC differentiation to CMs (Uosaki et al., 2011) with minimal modifications (see Experimental Procedures). We analyzed the temporal expression pattern of two representative CPC surface markers, KDR and PDGFRα, and found that the KDR$^+$PDGFRα$^+$ (KP) population (Kattman et al., 2011; Yang et al., 2008) prominently emerged from day 3 and peaked at day 5 in our system. To evaluate the cardiomyogenic potential of the KP population at different stages, we purified the KP population at days 3, 4, and 5 by fluorescence-activated cell sorting (FACS) and recultured the purified populations for 14 days in the absence of Wnt inhibitions (see Reculture Experiments) under serum-free condition (RPMI1640+B27 supplement) or under serum condition (RPMI1640+10% fetal bovine serum [FBS]) that permits diverse differentiation (Figures 1A, 1B, and S1A). In serum-free condition, the KP population at day 3 (KP-d3) efficiently gave rise to CMs (cardiac troponin T [cTnT$^+$]) as well as PDGFRβ$^+$ pericyte/mesenchymal cell (PC/MC) populations. KP-d4 and -d5 gave rise to more CMs and fewer PC/MCs than did KP-d3, suggesting that the KP population possesses differentiation potential to both CMs and PC/MCs and that the CM differentiation potential was enhanced at days 4 and 5. In serum condition, even though KP-d3 and -d4 possess CM differentiation potential in serum-free condition, KP-d3 and -d4 almost completely failed to differentiate into CMs, with >90% of the cells differentiating into PDGFRβ$^+$cTnT$^-$ PC/MCs. Alternatively, KP-d5 predominantly differentiated into CMs, even with serum (Figures 1A and 1B). These results indicate that the restriction of the fate determination to CMs in the KP population in this differentiation protocol occurs during days 4 to 5 of differentiation and that CFPs, which robustly differentiate into CMs even under serum condition, may presumably be included in KP-d5. These results are compatible with a previous study that showed insulin/insulin-like growth factor, which is found in serum, blocked CM differentiation during an early mesoderm stage (Freund et al., 2008).

To identify candidate cell-surface markers of CFPs in KP-d5, we employed a comprehensive analysis of global gene expression during differentiation days 3–5. We compared gene expression profiles among undifferentiated hiPSCs; purified KP-d3, -d4, -d5; and CMs induced from KP-d5 (Figure S1B). We identified 6 genes encoding cell-surface markers that showed significantly high deviation from the mean expression level of all genes on days 3, 4, or 5: integrin α5 chain (ITGA5; CD49e), kangai-1 (KAI1; CD82), PDGFRα (CD140a), tumor necrosis factor receptor superfamily 11A (TNFRSF11A; CD265), KDR (CD309), and jagged 1 (JAG1; CD339) (Figure 1C). Among them, only CD82 demonstrated a unique temporal change in its expression pattern, because it was upregulated >4-fold from days 4 to 5 and appeared to be significantly deviated from day 5, suggesting that CD82 is a potent candidate marker of CFPs. We examined the time course of CD82 expression during CM differentiation using flow cytometry. The CD82$^+$ population started to be observed from day 4, its percentage increased until day 7 (>60% at maximum), and gradually decreased thereafter (Figure 1D). The distinct appearance of the CD82$^+$ population within the PDGFRα$^+$ population at day 5 supported the possibility that CD82 is a specific cell-surface marker for CFPs.

CD82 Successfully Marks CFP Population *In Vitro*

Next, we examined the possibility that CD82 marks CFPs. We purified CD82$^+$ and CD82$^-$ cells among the PDGFRα$^+$CD13$^+$ CPC population (Ardehali et al., 2013) from days 3 to 7 by FACS (Figures S1C and S1D). From days 3 to 4, CD82$^-$ cells alone were purified; from day 5, both CD82$^-$ and CD82$^+$ cells were purified; and from days 6 to 7, CD82$^+$ cells alone were purified from PDGFRα$^+$CD13$^+$ cells. We recultured the purified populations without Wnt inhibitors and tested the differentiation potential and commitment of these populations toward CMs under serum-free or serum culture conditions. Under serum-free condition, CD82$^-$ cells (days 3–5) yielded cTnT$^+$ CMs with 50%–75% efficiency, and CD82$^+$ cells (days 5–7) yielded cTnT$^+$ CMs with 80%–95% efficiency. The rest of the cells were mainly PDGFRβ$^+$cTnT$^-$ PC/MCs. These results indicate that both the CD82$^+$ and CD82$^-$ populations in PDGFRα$^+$CD13$^+$ CPCs are potentially cardiomyogenic (Figures 2A and 2B). Under serum condition, CD82$^-$ cells did not differentiate into CMs; instead they predominantly differentiated into PDGFRβ$^+$cTnT$^-$ PC/MCs, indicating that CD82$^-$ cells can be differentiated into CM or non-CMs depending on the culture environment. Alternatively, CD82$^+$ cells predominantly differentiated into CMs independent of the culture conditions even with serum (Figures 2A and 2B). Of note, CD82$^-$ cells and CD82$^+$ cells at day 5 showed apparently distinct fate determination under serum condition. Immunostaining also showed that most CD82$^-$ cells at day 5 differentiated into nonbeating calponin$^+$ PC/MCs, whereas most CD82$^+$ cells differentiated into cTnT$^+$ CMs with

(C) Scattered dot plot analysis for the distribution of 288 CD genes at days 3, 4, and 5. The y axis is the log2 expression of the genes in the purified KP population. The x axis is the log2 ratio of the genes in the purified KP population compared with their average expression in undifferentiated iPSCs and CMs. The contour lines reflect the density of the gene distributions. ITGA5 (CD49e), KAI1 (CD82), PDGFRα (CD140a), TNFRSF11A (CD265), KDR (CD309), and JAG1 (CD339) showed significantly high deviations from the mean expression level of all genes on days 3, 4, or 5. Red dot indicates CD82.
(D) Representative flow cytometric analysis for CD82 and PDGFRα from days 0 to 15. Numbers in the quadrants represent the respective percentages of cells. See also Figures S1A and S1B.

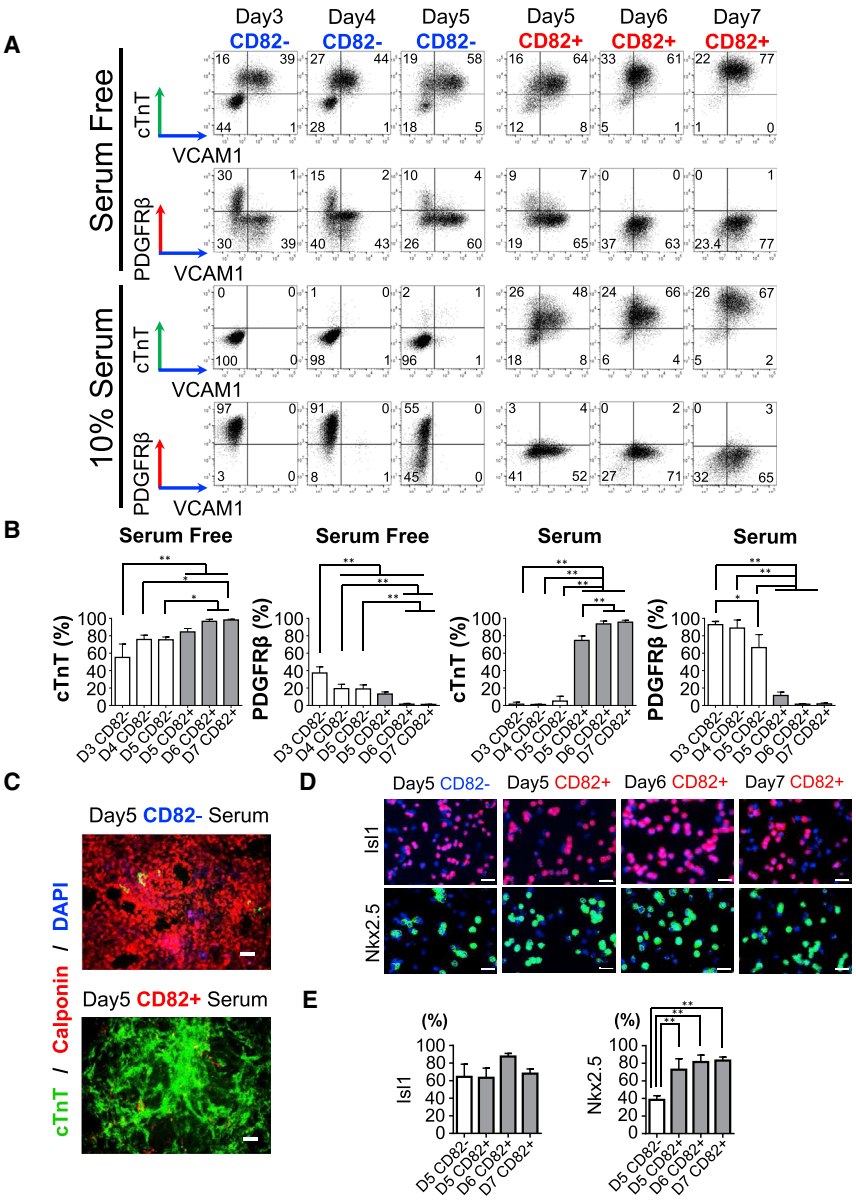

Figure 2. CD82 Successfully Marks CFP Population *In Vitro*

(A) Representative flow cytometric analysis of cTnT, PDGFRβ, and VCAM1. Purified CD82$^-$ or CD82$^+$ populations among the PDGFRα$^+$CD13$^+$ CPC population from days 3 to 7 were recultured for 14 days in the absence of Wnt inhibitors under serum-free (RPMI1640+B27 supplement) or serum condition (RPMI1640+10% FBS). Numbers in the quadrants represent the respective percentages of cells.

(B) Quantitative analysis of (A). Data are means ± SDs. *$p < 0.05$, **$p < 0.01$ by one-way ANOVA followed by Tukey's post hoc test ($n = 3$).

(C) Representative image of cTnT (green), calponin (red), and DAPI (blue) in differentiated cells derived from purified CD82$^-$ or CD82$^+$ populations among the PDGFRα$^+$CD13$^+$ CPC population at day 5 after 14 days' reculture under serum condition (RPMI1640+10% FBS) in the absence of Wnt inhibitors. DAPI, 4′,6-diamidino-2-phenylindole. Scale bars, 100 μm.

(D) Immunostaining of Isl1 (red), Nkx2.5 (green), and DAPI (blue) in purified CD82$^-$ or CD82$^+$ populations among the PDGFRα$^+$CD13$^+$ CPC population from days 5 to 7. Scale bars, 20 μm.

(E) Quantitative analysis of Isl1$^+$ and Nkx2.5$^+$ cells per nucleus in (D). Data are means ± SDs. *$p < 0.05$, **$p < 0.01$ by one-way ANOVA followed by Tukey's post hoc test ($n = 5$).

See also Figures S1C–S1G and S2–S4.

spontaneous beating even in serum condition (Figure 2C; Movies S1 and S2).

To further confirm the robustness of CD82$^+$ cells as CFPs restricted to CM fate, we examined CD82$^+$ cell differentiation to ECs. We purified KDR$^+$ cells among the PDGFRα$^+$ population, which was reported to possess EC differentiation potential (Ikuno et al., 2017; Prasain et al., 2014), segregated the KDR$^+$ cells into CD82$^-$ and CD82$^+$ cells, and cultured each population in an EC-oriented culture condition containing vascular endothelial cell growth factor (VEGF) from day 5 (Figures S1E–S1G). In the no-VEGF condition, both CD82$^-$ and CD82$^+$ populations differentiated into VE-cadherin$^+$ ECs at ~1% efficiency. In contrast, the induction of ECs from the CD82$^-$ population was increased by the addition of VEGF, but the EC appearance from the CD82$^+$ population did not increase (Figures S1F and S1G). These results indicated that CD82$^+$ cells no longer responded to EC differentiation cues.

We further compared CD82 expression with other mesoderm lineage markers. Two transcription factors, Isl1 and Nkx 2.5, which characterize CPCs (Moretti et al., 2006; Prall et al., 2007; Wu et al., 2006), were expressed in the majority of both CD82$^+$ and CD82$^-$ populations (Figures 2D and 2E). CD82$^-$ cells largely expressed Isl1 or Nkx2.5, suggesting that these transcription factors should be able to endow cardiomyogenic potential, but they do not immediately determine lineage commitment to CMs. The time course of CD82 expression revealed that CD82 is a CM progenitor stage-specific gene. CD82 expression and the CM markers cTnT and/or vascular cell adhesion molecule 1 (VCAM1) (Uosaki et al., 2011) at day 11 were largely mutually exclusive (Figure S2A), indicating that CD82 is expressed during the CM progenitor stage, but not in CMs. The expression of signal regulatory protein-α (SIRPA) (Dubois et al., 2011; Elliott et al., 2011) in mesoderm cells was first observed after CD82 expression (from day 7) and was gradually increased and maintained on CMs at day 11 (Figure S2B). The appearance (day 3) and peak (day 5) of CD13 expression preceded those of CD82. Most CD82$^+$ cells were CD13$^+$ until day 7 (Figure S2C). The mRNA expression time course further confirmed that CD82 is a CM progenitor

stage-restricted gene (Figure S2D) that is upregulated later than mesoderm genes (CD13, PDGFRα) and downregulated earlier than CM genes (SIRPA, VCAM1). All of these results indicate that CD82 is specifically expressed at the CM progenitor stage (late mesoderm before CMs) and determines single fate-restricted differentiation to CMs. One $CD82^+$ CFP was estimated to give rise to ~5.8 CMs after 14 days of reculture (Figure S2E). Action potentials of the CFP-derived CMs demonstrated that CFPs mainly give rise to ventricular-like CMs (action potential duration [APD]30-40/APD70-80 >1.5) with few nodal-like CMs (APD30-40/APD70-80 ≤1.5, dV/dt max < 10 V/s) (Ma et al., 2011) (Figures S3A and S3B). We examined the expression of CD82 and the cardiomyogenic potential of $CD82^-$ and $CD82^+$ cells in 2 other cell lines, 836B3 and 1201C1 (established by the episomal plasmid vector) (Okita et al., 2011, 2013) (Figure S4). Although the time course of the CM differentiation was slightly delayed in 836B3 and 1201C1 (Figures S4A and S4D), the CD82 expression pattern was almost similar to that in 201B6. Also similar to 201B6, $CD82^+$ cells in 836B3 and 1201C1 predominantly differentiated into CMs rather than into $CD90^+$ PC/MCs even under serum condition (Figures S4B, S4C, S4E, and S4F). These results indicate that CD82 can be used to isolate CFPs regardless of the original cell line or differentiation timing.

$CD82^+$ CFPs Overwhelmingly Give Rise to CMs *In Vivo*

To examine the CM-restricted differentiation of $CD82^+$ CFPs *in vivo*, we injected one of three different cell populations from hiPSCs ($CD13^+CD82^-$ CPCs at day 4, $VCAM1^+$ CMs at day 15, or $CD82^+$ CFPs at day 6) into the subrenal space of severe combined immunodeficiency (SCID) mice, which is a completely unrelated and independent environment from the heart (Figure 3A). Immunohistochemical staining with human nuclear antigen (HNA) (for all injected human cells) and cTnT at 1 or 2 weeks after injection revealed almost no engraftment of HNA^+ human cells after the injection of $CD13^+CD82^-$ CPCs (Figure 3B). Although a small number of $VCAM1^+$ CMs remained 1 week after injection (Figure 3B), the injected cells (HNA^+) disappeared 2 weeks after injection (data not shown). In contrast, much greater engraftment of HNA^+cTnT^+ human CMs was observed after the injection of $CD82^+$ CFPs (Figures 3B–3D). More than 99% of HNA^+ cells were positive for cTnT after the $CD82^+$ CFP injection (Figure 3C). These data indicate that $CD82^+$ CFPs survived well and almost exclusively differentiated into CMs even in a nonspecific environment *in vivo*. Next, we examined the engraftment of $CD82^+$ CFPs to infarcted hearts. We injected $CD82^+$ ($PDGFR\alpha^+CD13^+$) CFPs into the heart of a myocardial infarction model of nonobese diabetic (NOD)/NOD.Cg-Prkdcscid IL2rgtm1Sug/Jic (NOG) immunodeficient mice (Figure 3E). HNA^+cTnT^+ human CM clusters were successfully detected at 1 and 3 months after transplantation (Figure 3F). Striated sarcomeric structures, although still immature, formed in HNA^+cTnT^+ human CMs at 3 months after transplantation, suggesting structural maturation of the engrafted CMs (Figure 3J). Consistent with the results of the subrenal transplantation, CFPs primarily differentiated into CMs within the infarcted hearts at ~95% efficiency (1 month, 95.9% ± 2.4%; 3 months, 93.7% ± 2.7%) (Figure 3G). Fewer than 5% of neural/glial antigen 2 ($NG2)^+$ PCs were observed 1 and 3 months after transplantation (1 month, 3.6 ± 3.2%; 3 months, 2.3 ± 2.1%) (Figures 3H and 3I). These results indicate that hiPSC-derived $CD82^+$ CFPs can give rise predominantly to CMs after transplantation to the infarcted hearts, implying their application as a stable cardiomyogenic cell source for cardiac regeneration.

Exosome-Mediated Wnt/β-Catenin Signal Control through CD82 Expression

Next, we investigated the biological function of CD82 in CM differentiation. CD82 is recognized as an exosome marker. Additionally, it was reported to antagonize Wnt/β-catenin activity through the exosomal clearance of β-catenin from the cells (Chairoungdua et al., 2010). Wnt inhibition is known to potently induce differentiation and commitment to CMs from mesoderm cells (Naito et al., 2006; Yamashita et al., 2005). We speculated that CM commitment in $CD82^+$ cells may be regulated by Wnt inhibition through exosomal β-catenin clearance.

To test this hypothesis, we performed CD82 overexpression experiments. We established an hiPSC line carrying a tetracycline-inducible CD82/enhanced green fluorescent protein (EGFP) double-expressing vector based on the *piggyBac* transposon system (Woltjen et al., 2009) (Figure 4A). Doxycycline treatment (Dox+) in the hiPSC line robustly induced CD82/EGFP expression (Figures 4B and 4C). We collected the culture supernatant and the nuclear and cytoplasmic fractions of cells treated under Dox+ or Dox- conditions. Although the cell number was significantly lower in Dox+ condition (Figure 4D), the number of exosome particles was approximately 5.2 times higher in Dox+ supernatant than that in Dox- (Figures 4E and 4F). Western blot analysis adjusted to the exosome number revealed that β-catenin was much more highly contained in Dox+ exosomes compared to Dox- exosomes (Figure 4G), suggesting that CD82 overexpression enhanced the secretion of exosomes containing β-catenin. Although no clear difference was observed in the β-catenin level in the cytoplasm (Figure 4H), nuclear β-catenin protein was significantly decreased in Dox+ cells (Figure 4I). In addition, canonical Wnt signal activity was significantly reduced in Dox+ cells (Figure 4J).

Functional Significance of CD82 Expression during CM Differentiation from CPCs

Finally, we investigated the biological function of CD82 in CM differentiation from mesoderm cells. We performed CD82 overexpression experiments in $PDGFR\alpha^+$ CPCs at day 5 (Figure 5A). Purified $PDGFR\alpha^+$ cells were recultured with serum under one of the following conditions for 2 days (days 5–7): (1) Dox- (negative control), (2) Dox- with Wnt inhibitors (XAV 5 μM + IWP4 2.5 μM) (positive control), or (3) Dox+ with no Wnt inhibitors. CD82 expression was successfully induced by Dox+ (Figures 5B and 5C). Wnt signal activation was significantly suppressed by either Wnt inhibitors or CD82 overexpression (Dox+) (Figure 5D). We collected the culture supernatant and the nuclear and cytoplasmic fractions of cells. The increase in the number of exosome particles in Dox+ supernatant was approximately 3.6 and 2.8 times higher than that in Dox- and Dox- with Wnt inhibitors supernatants, respectively (Figures 5E and 5F). Western blot analysis adjusted by the exosome number revealed that

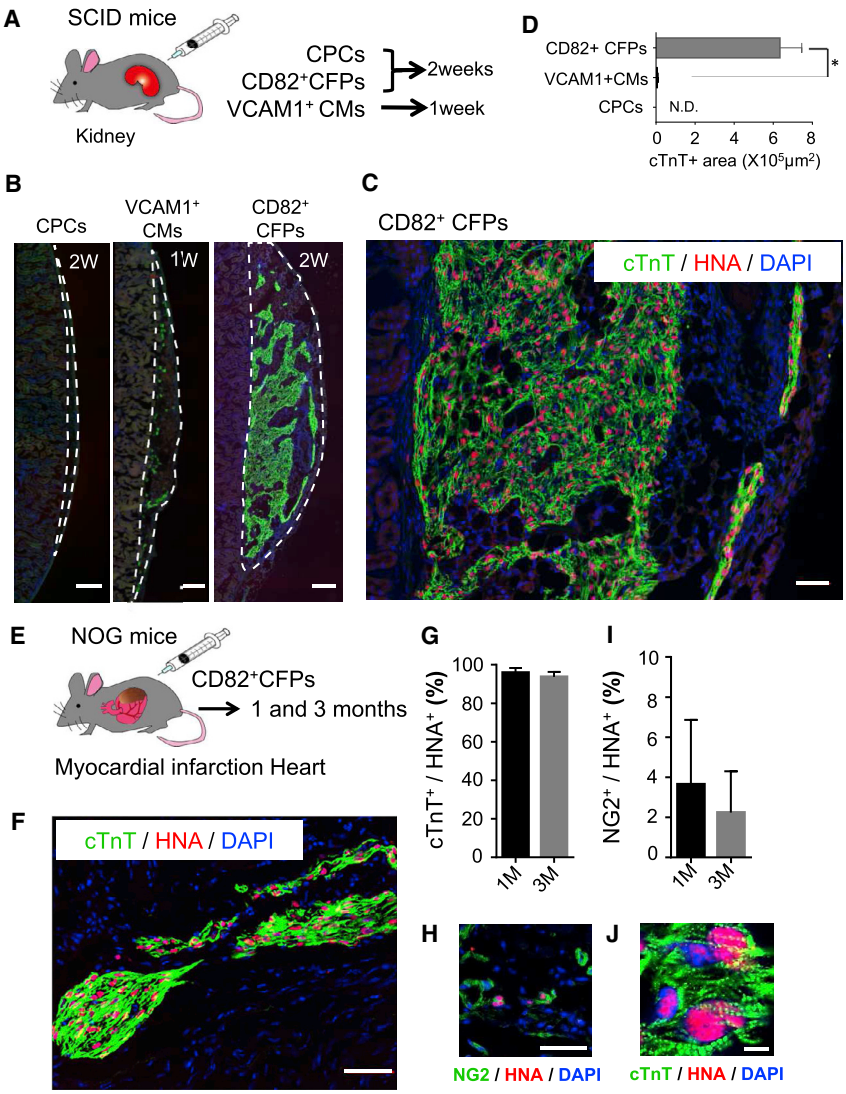

Figure 3. CD82⁺ CFPs Overwhelmingly Give Rise to CMs *In Vivo*

(A) Schematic representation of the cell transplantation into subrenal space of SCID mice. $CD13^+CD82^-$ CPCs at day 4, $CD82^+$ CFPs at day 6, or $VCAM1^+$ CMs at day 15 were purified with MACS and transplanted. Kidneys were collected 2 weeks after transplantation ($CD13^+CD82^-$ CPCs and $CD82^+$ CFPs) or 1 week after transplantation ($VCAM1^+$ CMs).

(B) Representative images of cTnT (green), human nuclear antigen (HNA (red). and DAPI (blue) staining after transplantation of $CD13^+CD82^-$ CPCs (2 weeks), $CD82^+$ CFPs (2 weeks), and $VCAM1^+$ CMs (1 week). White dashed lines indicate the injected region. Scale bars, 200 μm.

(C) Higher magnification image of cTnT (green), HNA (red), and DAPI (blue) after transplantation of $CD82^+$ CFPs. Note that almost all of the HNA^+-transplanted cells are positive for cTnT. Scale bar, 200 μm.

(D) cTnT-positive area after transplantation of $CD13^+CD82^-$ CPCs, $CD82^+$ CFPs, or $VCAM1^+$ CMs. N.D., not detected. Data are means ± SDs. *$p < 0.05$ by Mann-Whitney test ($n = 4$, 5 different slides per animal, 4 animals).

(E) Schematic representation of the transplantation of FACS-purified $CD82^+$ CFPs ($PDGFR\alpha^+CD13^+$) into the heart of a myocardial infarction model of NOG immunodeficient mice. Hearts were collected 1 and 3 months after transplantation.

(F) Representative image of cTnT (green), HNA (red), and DAPI (blue) staining 3 months after the transplantation of $CD82^+$ CFPs. Scale bar, 50 μm.

(G) Percentage of $cTnT^+$ cells among HNA^+ cells at 1 and 3 months after transplantation. Data are means ± SDs ($n = 3$, 4 different slides per animal, 3 animals).

(H) Representative image of NG2 (green), HNA (red), and DAPI (blue) staining 3 months after the transplantation of $CD82^+$ CFPs. Scale bar, 50 μm.

(I) Quantification of $NG2^+$ cells per HNA^+ cells at 1 and 3 months after transplantation. Data are means ± SDs ($n = 3$, 4 different slides per animal, 3 animals).

(J) Higher magnification image of cTnT (green), HNA (red), and DAPI (blue) staining 3 months after transplantation of $CD82^+$ CFPs. Sarcomere-like structure is observed. Scale bar, 5 μm.

β-catenin and CD82 were much more contained in Dox+ exosomes compared to those in Dox- or Dox- with Wnt inhibitor-treated exosomes (Figures 5G and 5H), indicating that CD82 overexpression contributed to the increase in exosome-mediated β-catenin secretion. Although no clear difference was observed in β-catenin levels in the cytoplasm among the 3 groups (Figure 5I), the nuclear β-catenin protein level was significantly decreased in Dox+ or Dox- with Wnt inhibitor-treated cells (Figure 5J). We further confirmed that CM differentiation at 14 days after reculture was significantly enhanced by CD82 overexpression (Figures 5K and 5L). These results suggest a biological function of CD82 in cardiomyogenesis from $PDGFR\alpha^+$ cells; i.e., CD82 attenuates Wnt signaling through the exosomal clearance of nuclear β-catenin in CPCs, resulting in augmented CM differentiation through commitment to CMs.

DISCUSSION

In the present study, we found that human CFPs, a hiPSC-derived cell population that almost exclusively differentiates into CMs under diverse conditions *in vitro* and *in vivo*, are marked by the cell-surface molecule CD82. Furthermore, we found that CD82 contributes to CM differentiation by attenuating the Wnt/β-catenin signaling pathway through exosomal regulation.

The significance of CFPs is schematically shown in Figure 6. The differentiation potential of undifferentiated PSCs is broad over three germ layer cells. Even though PSCs can give rise to CMs in CM-specific culture conditions, they can be differentiated into all germ layer derivatives *in vivo* (nonspecific conditions), leading to teratoma formation. CPCs have restricted

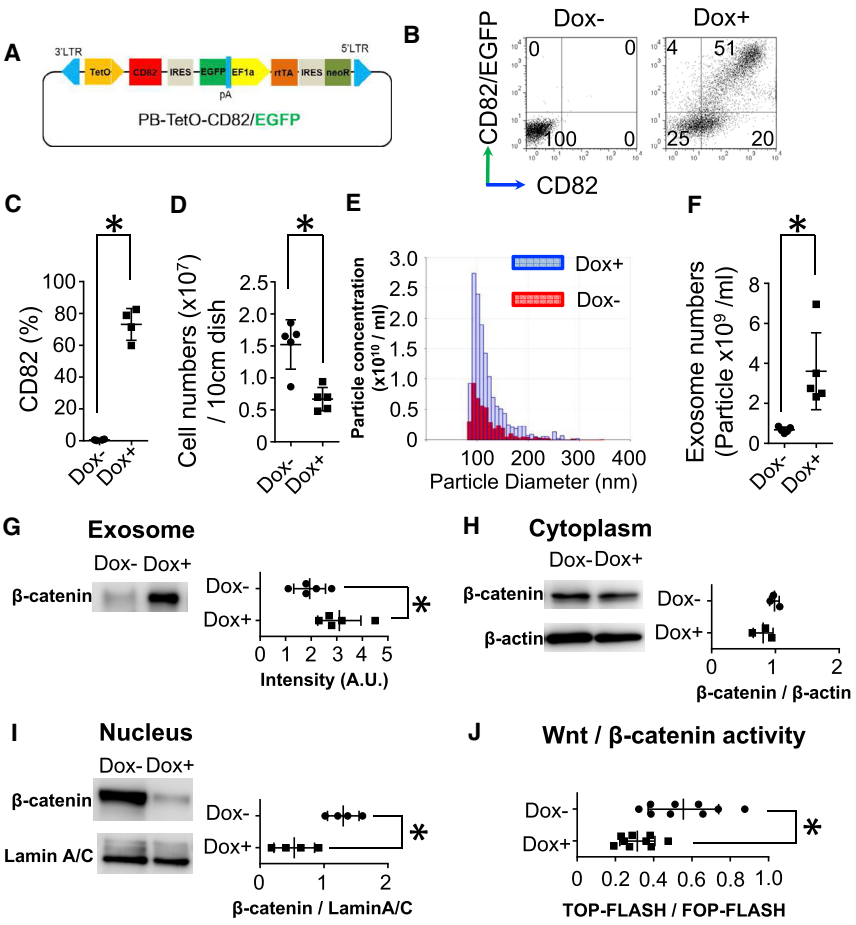

Figure 4. Exosome-Mediated Wnt/β-Catenin Signal Control through CD82 Expression

(A) Construct of the Tet-inducible CD82/EGFP expressing *piggyBac* vector (PB-TetO-CD82/EGFP vector).

(B) Representative flow cytometric analysis of EGFP and CD82 (Alexa Fluor 647) expression in the iPSC line under doxycycline (Dox)+ or Dox- condition for 3 days. Numbers in the quadrants represent the respective percentages of cells.

(C) Quantitative analysis of $CD82^+$ cells under Dox+ or Dox- condition for 3 days. Data are means ± SDs. *$p < 0.05$ by Mann-Whitney test ($n = 4$).

(D) Cell numbers under Dox+ or Dox- condition for 3 days. Cells at subconfluency in a 10-cm dish were exposed to Dox+ or Dox- condition for 3 days. Data are means ± SDs. *$p < 0.05$ by Mann-Whitney test ($n = 5$).

(E) Representative exosome particle number and size distribution under Dox+ or Dox- condition for 3 days. The x axis indicates particle diameter (nanometers), and the y axis indicates particle concentration (× 10^{10}/mL). Particle size distribution and particle concentration were analyzed after ultracentrifugation. Blue and red boxes indicate exosome particles under Dox+ or Dox- condition, respectively, for 3 days.

(F) Exosome numbers in 1 mL of supernatant under Dox+ or Dox- condition for 3 days. Total number of exosomes was calculated by multiplying the measured exosome concentration by the volume and then dividing by the initially collected supernatant volume (8 mL). Data are means ± SDs. *$p < 0.05$ by Mann-Whitney test ($n = 5$).

(G) β-Catenin in exosomes. Representative western blot of β-catenin in an exosome (left panel) and quantitative evaluation of β-catenin intensity under Dox+ or Dox- condition (right panel). Sample loading amounts were adjusted with exosome numbers. A.U., arbitrary units. *$p < 0.05$ by Mann-Whitney test ($n = 5$).

(H) Representative western blot of β-catenin in the cytoplasmic fraction (left panel) and β-catenin intensity normalized to β-actin under Dox+ or Dox- condition (right panel). *$p < 0.05$ by Mann-Whitney test ($n = 3$).

(I) Representative western blot of β-catenin in the nuclear fraction (left panel) and β-catenin intensity normalized to Lamin A/C under Dox+ or Dox- condition (right panel). *$p < 0.05$ by Mann-Whitney test ($n = 4$).

(J) Canonical Wnt signal activity. TOP-FLASH/FOP-FLASH ratio with or without Dox. *$p < 0.05$ by Mann-Whitney test ($n = 9$).

differentiation potential to mesoderm cell lineages, which largely give rise to CMs under CM-specific culture conditions. Nevertheless, in nonspecific conditions, CPCs exhibit broader differentiation capacity, resulting in the appearance of various mesoderm derivatives that may not include CMs (Lalit et al., 2016; Yamashita, 2016). In contrast to undifferentiated PSCs or CPCs, $CD82^+$ CFPs have privileged differentiation potential in which the direction of differentiation is almost exclusively limited to CMs even under nonspecific conditions and *in vivo*. Consequently, $CD82^+$ CFPs can differentiate into CMs specifically and stably *in vivo* after transplantation.

The identification of cell-surface markers associated with cardiomyogenic potential has been a high priority in cardiac regeneration research because of the potential broad application of cells without genetic modification (Anderson et al., 2007). Although numerous cell-surface markers, including ROR2, CD13, HCN4, SSEA1, GFRA2, KDR, and PDGFRα, have been identified during hiPSC differentiation toward CMs, all of these markers specified mesoderm cells or CPCs that give rise not only to CMs but also to non-CMs, including vascular cells or stromal cells (Ardehali et al., 2013; Blin et al., 2010; Burridge et al., 2012; Ishida et al., 2016; Kattman et al., 2011; Später et al., 2013; Yang et al., 2008). SIRPA is another cell-surface marker reported to be expressed on CMs and CM progenitor populations (Dubois et al., 2011; Elliott et al., 2011). However, the exclusive differentiation of $SIRPA^+$ progenitors to CMs is still unclear. In addition, SIRPA is expressed in both CM progenitors and CMs. Thus, the present study successfully demonstrates a cell-surface marker, CD82, that identifies the CFP population. With the use of CD82, we can easily detect and obtain a pure human cell population that specifically gives rise to CMs.

In contrast to previous reports that demonstrated fair engraftment of CPCs as well as CMs into hearts (Chong et al., 2014; Laflamme et al., 2007), we observed no or poor engraftment of $CD13^+CD82^-$ CPCs and $VCAM1^+$ CMs in subrenal space. These results may suggest that CM engraftment, survival, and differentiation is dependent on the microenvironment of the injected

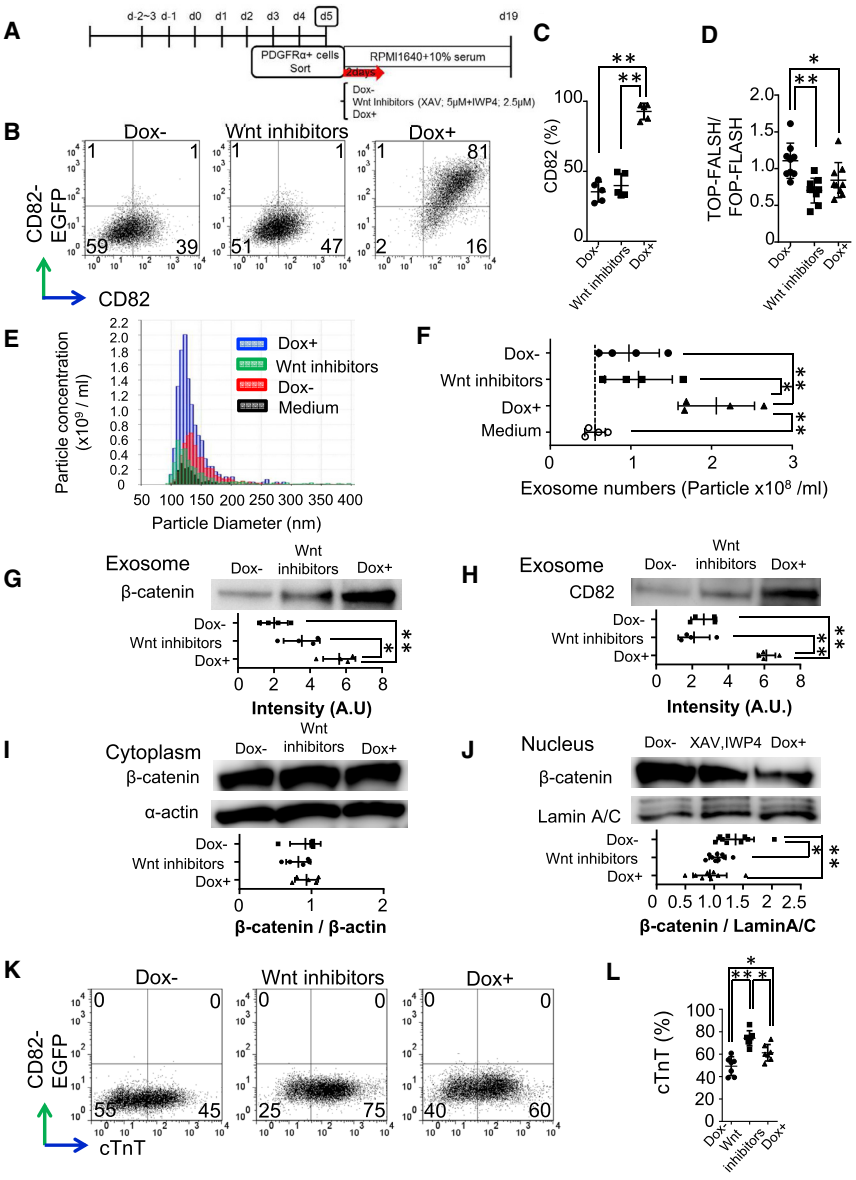

Figure 5. Functional Significance of CD82 Expression during CM Differentiation from CPCs

(A) Schematic protocol for recultured experiments of purified PDGFRα$^+$ populations at day 5 derived from an hiPSC line carrying a tetracycline-inducible CD82/EGFP double-expressing vector. Purified PDGFRα$^+$ mesoderm cells were recultured with serum (10% FBS) under one of the following conditions for 2 days (days 5–7): (1) Dox- (negative control), (2) Dox- with Wnt inhibitors (XAV 5 μM + IWP4 2.5 μM) (positive control), or (3) Dox+ with no Wnt inhibitors.

(B) Representative flow cytometric analysis of EGFP and CD82 (Alexa Fluor 647) expression in the purified PDGFRα$^+$ population under Dox+, Dox-, or Wnt inhibitors condition for 2 days. Numbers in the quadrants represent the respective percentages of cells.

(C) Quantitative analysis of CD82$^+$ cells in (B). Data are means ± SDs. **p < 0.01 by one-way ANOVA followed by Tukey's post hoc test (n = 5).

(D) Canonical Wnt signal activity. TOP-FLASH/FOP-FLASH under Dox+, Dox-, or Wnt inhibitors condition for 2 days. Data are means ± SDs. **p < 0.01, *p < 0.05 by one-way ANOVA followed by Tukey's post hoc test (n = 9).

(E) Representative exosome particle number and size distribution under Dox+, Dox-, or Wnt inhibitors condition for 2 days. The x axis indicates particle diameter (nanometers), and the y axis indicates particle concentration (× 10^9/mL). Particle size distribution and particle concentration were analyzed after ultracentrifugation. Black, blue, red, and green boxes indicate exosome particles in medium (RPMI1640+10% FBS), Dox+, Dox-, or Wnt inhibitors condition for 2 days, respectively.

(F) Exosome numbers in 1 mL of supernatant of medium (RPMI1640+10% FBS), Dox+, Dox-, or Wnt inhibitors condition for 2 days. Total number of exosome was calculated by multiplying the measured exosome concentration by the volume and then dividing by the initial collected supernatant volume (4 mL). Dashed line indicates the number of exosomes in the medium. Data are means ± SDs. *p < 0.05 by Mann-Whitney test (n = 4).

(G) β-Catenin in exosomes. Representative western blot of β-catenin in an exosome (upper panel) and quantitative evaluation of β-catenin intensity in Dox+, Dox-, or Wnt inhibitors condition for 2 days (lower panel). Sample loading amounts were adjusted with the exosome number. A.U., arbitrary units. *p < 0.05, **p < 0.01 by one-way ANOVA post hoc Tukey's test (n = 4).

(H) CD82 in exosomes. Representative western blot of β-catenin in an exosome (upper panel) and quantitative evaluation of β-catenin intensity in Dox+, Dox-, or Wnt inhibitors condition for 2 days (lower panel). Sample loading amounts were adjusted with the exosome number. A.U., arbitrary units. *p < 0.05, **p < 0.01 by one-way ANOVA post hoc Tukey's test (n = 4).

(I) Representative western blot of β-catenin and β-actin in the cytoplasmic fraction (upper panels) and β-catenin intensity normalized to β-actin in Dox+, Dox-, or Wnt inhibitors condition for 2 days (lower panel) (n = 5).

(J) Representative western blot of β-catenin and Lamin A/C in the nuclear fraction (upper panels) and β-catenin intensity normalized to Lamin A/C in Dox+, Dox-, or Wnt inhibitors condition for 2 days (lower panel). *p < 0.05, **p < 0.01 by one-way ANOVA followed by Tukey's post hoc test (n = 9).

(K) Representative flow cytometric analysis of EGFP and cTnT expression 14 days after reculture. Numbers in the quadrants represent the respective percentages of cells.

(L) Quantitative analysis of cTnT$^+$ cells in (L). Data are means ± SDs. *p < 0.05, **p < 0.01 by one-way ANOVA followed by Tukey's post hoc test (n = 7).

sites. Even when injected into subrenal space, which is unlikely a niche dedicated to cardiac cell lineages, CD82$^+$ CFPs engrafted as CMs, suggesting that CD82$^+$ CFPs may possess robust adaptability to various microenvironments. Although a previous report found a podoplanin-positive cardiac progenitor population mainly differentiated into pacemaker-like cells (Birket et al., 2015), CD82$^+$ CFPs predominantly differentiated into ventricular CMs (Figures S3A and S3B), which may be suitable

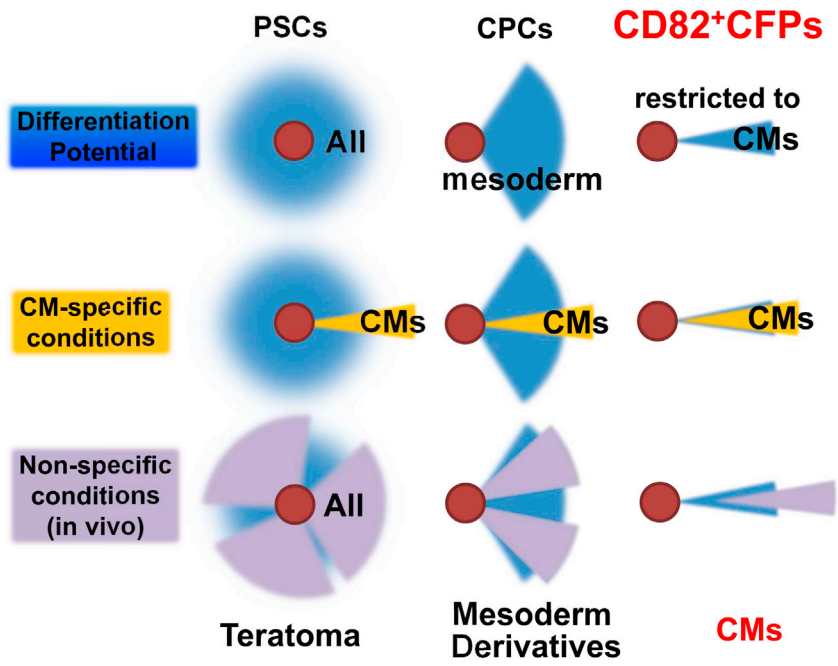

Figure 6. Differentiation Spectrum of PSCs, CPCs, and CD82$^+$ CFPs

Schematic diagrams of the differentiation potential spectrum (blue, all rows) and differentiation abilities under CM-specific (yellow, middle row) or nonspecific conditions, including after *in vivo* transplantation (purple, bottom row). Undifferentiated PSCs (left column), CPCs (central column) and CD82$^+$ CFPs (right column) are shown. Note that only CFPs, whose differentiation potential is restricted to CMs, can overwhelmingly differentiate into CMs even under nonspecific conditions.

to compensate damaged myocardium. Taking these results together, although further refinement of the transplantation efficiency in combination with other cell and tissue transplantation technologies is required, CD82$^+$ CFPs may serve as a potential candidate for cardiac regenerative cell therapy.

Recently, CD82 was reported to be expressed on hematopoietic stem cells and skeletal muscle satellite cells (Alexander et al., 2016; Hur et al., 2016; Uezumi et al., 2016). However, the involvement of Wnt signaling and exosome regulation in CD82 function was not described in those reports. In addition, CD82 was expressed in completely different developmental stages and tissues from CFPs, suggesting that previously described CD82$^+$ populations are different from the population reported here and have distinct functions. Wnt inhibition is crucial for the CM commitment process (Naito et al., 2006; Yamashita et al., 2005). The present study suggests a molecular mechanism in which CD82-mediated exosomal regulation contributes to CM fate determination. In addition, we show that the expression of the cardiac transcription factors Isl1 and Nkx2.5 is still insufficient to exclusively determine CM fate (Figures 2D and 2E), suggesting that other mechanisms, including epigenetic regulation, are required. The molecular and mechanical links among CD82, exosome, and epigenome are critical research targets for future study.

In conclusion, CD82 may provide a valuable clue to elucidating the CM fate determination process and offers an efficient way to prepare an almost pure CFP population from human PSCs. Our findings broadly extend to basic and applied stem cell biology in the cardiac field.

EXPERIMENTAL PROCEDURES

Further details are given in the Supplemental Experimental Procedures.

Human iPSC Culture and CM Differentiation

The hiPSC line 201B6 (4 factors [Oct3/4, Sox2, Klf4, and c-Myc] from skin adult fibroblast) (Takahashi et al., 2007) was used as a representative human iPSC line in all of the experiments unless stated otherwise. The hiPSCs maintenance culture method was reported previously (Laflamme et al., 2007; Masumoto et al., 2014; Uosaki et al., 2011).

The CM differentiation protocol also was reported previously (Laflamme et al., 2007; Masumoto et al., 2014; Uosaki et al., 2011), with minimal modifications. We used RPMI1640+B27 supplement (insulin+) medium from day 5, instead of RPMI1640+B27 supplement without insulin (insulin-) medium.

Reculture Experiments

Differentiated cells were recultured in the absence of Wnt inhibitions under serum-free condition (RPMI1640+B27 supplement [insulin+] or under serum condition (RPMI1640+10% FBS) with the addition of 10 mM Y-27632 (Wako; for the first 2 days after plating) and penicillin and streptomycin (Meiji Seika Pharma). The culture medium was refreshed every 2 days (Figures 1 and 2).

Microarray Analysis

RNA was extracted from undifferentiated iPSCs; purified KP cells at days 3, 4, and 5, and CMs derived from KP cells at day 5 under serum condition (Figure S1B) using the RNeasy Mini Kit (Qiagen). Total RNA was reverse transcribed into cDNA via SuperScript II Reverse Transcriptase (Life Technologies). Samples were labeled with Cy3 using the BioArray HighYield RNA Transcript Labeling Kit (T7) (Enzo Life Sciences). Labeled cDNA was hybridized with Human Genome U133 Plus 2.0 Array by the GeneChip Hybridization Control Kit and the GeneChip Fluidics Station 450 (all Affymetrix) at 45°C for 16 hr. Arrays were scanned with the GeneChip Scanner 3000 7G according to the manufacturer's protocol and analyzed using GeneChip operating software (both Affymetrix). The raw data were normalized using the MAS5 algorithm (median score of the gene expressions: 500).

Animal Model Preparation and Transplantation

All of the animal experiments were approved by the Kyoto University Animal Experimentation Committee and performed in accordance with the guidelines for Animal Experiments of Kyoto University, which conforms to Japanese law and the *Guide for the Care and Use of Laboratory Animals*.

Male immunodeficient mice (SCID C.B17/Icr-scid/scid Jcl mice [CLEA Japan] or NOG, CLEA Japan) aged 8–12 weeks were used for transplantation into subrenal space or hearts of a myocardial infarction model. Then, 2×10^6 CD82$^+$ CFPs purified with FACS were suspended in 20 μL RPMI1640 medium and injected into the left ventricular myocardium directly after left anterior descending (LAD) coronary ligation of NOG mice. Finally, 5×10^6 CD13$^+$ CD82$^-$ CPCs, CD82$^+$ CFPs, and VCAM1$^+$ CMs purified with magnetic-activated cell sorting (MACS) were suspended in 20 μL of RPMI1640 medium and injected into the subrenal space of SCID mice.

Isolation and Quantification of Exosome

Undifferentiated tetO-CD82-EGFP iPSCs at subconfluency in a 10-cm dish were cultured in primate ESC medium (ReproCELL) with 10 ng/mL basic fibroblast growth factor (bFGF) with or without 1 μg/mL Dox for 3 consecutive days. PDGFRα$^+$ cells at day 5 were recultured in a 6-well plate with serum (10% FBS) under one of the following conditions for 2 days (days 5–7): (1) Dox- (negative control), (2) Dox- with Wnt inhibitors (XAV 5 μM + IWP4 2.5 μM) (positive control), or (3) Dox+ with no Wnt inhibitors. The collected supernatant was centrifuged at 2,000*g* for 30 min to remove cells and at 12,000*g* for 1 hr to remove debris. Cell-free supernatant was passed through a 0.22-mm pore filter (Merck Millipore) and finally submitted to ultracentrifugation at 100,000 *g* (Beckman Coulter Optima L-100XP ultracentrifuge, Beckman Coulter) for 1 hr at 4°C. After discarding the supernatant, pellets were eluted in PBS with 40 mM HEPES and 100 mM KCl (100–200 μL) and analyzed.

Western Blotting

Nuclear and cytoplasmic fractions were extracted from undifferentiated iPSCs with the NE-PER Nuclear and Cytoplasmic Extraction Reagents Kit (Thermo Fisher Scientific). Exosomes were lysated with radioimmunoprecipitation assay (RIPA) buffer (Thermo Fisher Scientific) and supplemented with protease inhibitor cocktail (Roche). The protein concentration was quantified by the Protein Assay Bicinchoninate Kit (Nacalai Tesque). Equal amounts of proteins from the nuclear and cytoplasmic fractions and proteins from exosomes adjusted with exosome particle numbers were examined for western blotting.

DATA AND SOFTWARE AVAILABILITY

The accession number for the microarray data reported in this paper is Gene Expression Omnibus: GSE90000. The accession numbers for the flow cytometry data reported in this paper is Flow Repository: FR-FCM-ZYEA, -ZYDL, -ZYDM, -ZYDN, -ZYDX, -ZYDP, -ZYDQ, -ZYDR, -ZYDS, -ZYDT, -ZYDU, -ZYDV, -ZYEY, -ZYE2, and -ZYE3. The accession number for the full-length human CD82 cDNA reported in this paper is NCBI: NM_002231.

SUPPLEMENTAL INFORMATION

Supplemental Information includes Supplemental Experimental Procedures, four figures, two tables, and two movies and can be found with this article online at https://doi.org/10.1016/j.celrep.2017.12.057.

ACKNOWLEDGMENTS

We thank Dr. S. Yamanaka (Center for iPS Cell Research and Application, Kyoto University) for research grants (102134400011) from the Core Center for iPS Cell Research, Research Center Network for Realization of Regenerative Medicine from the Japan Agency for Medical Research and Development. This work was supported by research grants from the Ministry of Education, Science, Sports and Culture of Japan (15H04819, 26860554, 16K19402) and Uehara Life Science (203134400011). We thank Mr. Miyake, Ms. Hirata, Ms. Yoshioka, and Ms. Takei for technical assistance and Dr. Peter Karagiannis (Kyoto University) for critical reading of the manuscript.

AUTHOR CONTRIBUTIONS

M.T. designed and conducted the experiments and analyzed the data. Y.K., H.M., S.F., T.H., H.F., A.I.-T., Y.M., and T.S. conducted the experiments. H.M. and Y.Y. supervised the animal experiments. M.T., H.M., and J.K.Y. wrote the main manuscript text. J.K.Y. supervised the project. All of the authors reviewed and approved the manuscript.

DECLARATION OF INTERESTS

J.K.Y. is a founder of iHeart Japan Corporation and is a member of its scientific advisory board. The remaining authors declare no conflicts of interest. The patents related to this article are WO2015166638 A1, CN106459922A, EP3138906A1, and US20170067023.

Received: August 26, 2017
Revised: October 22, 2017
Accepted: December 17, 2017
Published: January 9, 2018

REFERENCES

Alexander, M.S., Rozkalne, A., Colletta, A., Spinazzola, J.M., Johnson, S., Rahimov, F., Meng, H., Lawlor, M.W., Estrella, E., Kunkel, L.M., and Gussoni, E. (2016). CD82 is a marker for prospective isolation of human muscle satellite cells and is linked to muscular dystrophies. Cell Stem Cell *19*, 800–807.

Anderson, D., Self, T., Mellor, I.R., Goh, G., Hill, S.J., and Denning, C. (2007). Transgenic enrichment of cardiomyocytes from human embryonic stem cells. Mol. Ther. *15*, 2027–2036.

Ardehali, R., Ali, S.R., Inlay, M.A., Abilez, O.J., Chen, M.Q., Blauwkamp, T.A., Yazawa, M., Gong, Y., Nusse, R., Drukker, M., and Weissman, I.L. (2013). Prospective isolation of human embryonic stem cell-derived cardiovascular progenitors that integrate into human fetal heart tissue. Proc. Natl. Acad. Sci. USA *110*, 3405–3410.

Birket, M.J., Ribeiro, M.C., Verkerk, A.O., Ward, D., Leitoguinho, A.R., den Hartogh, S.C., Orlova, V.V., Devalla, H.D., Schwach, V., Bellin, M., et al. (2015). Expansion and patterning of cardiovascular progenitors derived from human pluripotent stem cells. Nat. Biotechnol. *33*, 970–979.

Blin, G., Nury, D., Stefanovic, S., Neri, T., Guillevic, O., Brinon, B., Bellamy, V., Rücker-Martin, C., Barbry, P., Bel, A., et al. (2010). A purified population of multipotent cardiovascular progenitors derived from primate pluripotent stem cells engrafts in postmyocardial infarcted nonhuman primates. J. Clin. Invest. *120*, 1125–1139.

Burridge, P.W., Keller, G., Gold, J.D., and Wu, J.C. (2012). Production of de novo cardiomyocytes: human pluripotent stem cell differentiation and direct reprogramming. Cell Stem Cell *10*, 16–28.

Burridge, P.W., Matsa, E., Shukla, P., Lin, Z.C., Churko, J.M., Ebert, A.D., Lan, F., Diecke, S., Huber, B., Mordwinkin, N.M., et al. (2014). Chemically defined generation of human cardiomyocytes. Nat. Methods *11*, 855–860.

Chairoungdua, A., Smith, D.L., Pochard, P., Hull, M., and Caplan, M.J. (2010). Exosome release of β-catenin: a novel mechanism that antagonizes Wnt signaling. J. Cell Biol. *190*, 1079–1091.

Chong, J.J., Yang, X., Don, C.W., Minami, E., Liu, Y.W., Weyers, J.J., Mahoney, W.M., Van Biber, B., Cook, S.M., Palpant, N.J., et al. (2014). Human embryonic-stem-cell-derived cardiomyocytes regenerate non-human primate hearts. Nature *510*, 273–277.

Dong, J.T., Lamb, P.W., Rinker-Schaeffer, C.W., Vukanovic, J., Ichikawa, T., Isaacs, J.T., and Barrett, J.C. (1995). KAI1, a metastasis suppressor gene for prostate cancer on human chromosome 11p11.2. Science *268*, 884–886.

Dubois, N.C., Craft, A.M., Sharma, P., Elliott, D.A., Stanley, E.G., Elefanty, A.G., Gramolini, A., and Keller, G. (2011). SIRPA is a specific cell-surface marker for isolating cardiomyocytes derived from human pluripotent stem cells. Nat. Biotechnol. *29*, 1011–1018.

Elliott, D.A., Braam, S.R., Koutsis, K., Ng, E.S., Jenny, R., Lagerqvist, E.L., Biben, C., Hatzistavrou, T., Hirst, C.E., Yu, Q.C., et al. (2011). NKX2-5(eGFP/w) hESCs for isolation of human cardiac progenitors and cardiomyocytes. Nat. Methods *8*, 1037–1040.

Freund, C., Ward-van Oostwaard, D., Monshouwer-Kloots, J., van den Brink, S., van Rooijen, M., Xu, X., Zweigerdt, R., Mummery, C., and Passier, R. (2008). Insulin redirects differentiation from cardiogenic mesoderm and endoderm to neuroectoderm in differentiating human embryonic stem cells. Stem Cells *26*, 724–733.

Hur, J., Choi, J.I., Lee, H., Nham, P., Kim, T.W., Chae, C.W., Yun, J.Y., Kang, J.A., Kang, J., Lee, S.E., et al. (2016). CD82/KAI1 maintains the dormancy of long-term hematopoietic stem cells through interactions with DARC-expressing macrophages. Cell Stem Cell *18*, 508–521.

Ikuno, T., Masumoto, H., Yamamizu, K., Yoshioka, M., Minakata, K., Ikeda, T., Sakata, R., and Yamashita, J.K. (2017). Efficient and robust differentiation of endothelial cells from human induced pluripotent stem cells via lineage control with VEGF and cyclic AMP. PLoS ONE *12*, e0173271.

Ishida, H., Saba, R., Kokkinopoulos, I., Hashimoto, M., Yamaguchi, O., Nowotschin, S., Shiraishi, M., Ruchaya, P., Miller, D., Harmer, S., et al. (2016). GFRA2 identifies cardiac progenitors and mediates cardiomyocyte differentiation in a RET-independent signaling pathway. Cell Rep. *16*, 1026–1038.

Kattman, S.J., Witty, A.D., Gagliardi, M., Dubois, N.C., Niapour, M., Hotta, A., Ellis, J., and Keller, G. (2011). Stage-specific optimization of activin/nodal and BMP signaling promotes cardiac differentiation of mouse and human pluripotent stem cell lines. Cell Stem Cell *8*, 228–240.

Laflamme, M.A., Chen, K.Y., Naumova, A.V., Muskheli, V., Fugate, J.A., Dupras, S.K., Reinecke, H., Xu, C., Hassanipour, M., Police, S., et al. (2007). Cardiomyocytes derived from human embryonic stem cells in pro-survival factors enhance function of infarcted rat hearts. Nat. Biotechnol. *25*, 1015–1024.

Lalit, P.A., Salick, M.R., Nelson, D.O., Squirrell, J.M., Shafer, C.M., Patel, N.G., Saeed, I., Schmuck, E.G., Markandeya, Y.S., Wong, R., et al. (2016). Lineage reprogramming of fibroblasts into proliferative induced progenitor cells by defined factors. Cell Stem Cell *18*, 354–367.

Ma, J., Guo, L., Fiene, S.J., Anson, B.D., Thomson, J.A., Kamp, T.J., Kolaja, K.L., Swanson, B.J., and January, C.T. (2011). High purity human-induced pluripotent stem cell-derived cardiomyocytes: electrophysiological properties of action potentials and ionic currents. Am. J. Physiol. Heart Circ. Physiol. *301*, H2006–H2017.

Masumoto, H., Ikuno, T., Takeda, M., Fukushima, H., Marui, A., Katayama, S., Shimizu, T., Ikeda, T., Okano, T., Sakata, R., and Yamashita, J.K. (2014). Human iPS cell-engineered cardiac tissue sheets with cardiomyocytes and vascular cells for cardiac regeneration. Sci. Rep. *4*, 6716.

Moretti, A., Caron, L., Nakano, A., Lam, J.T., Bernshausen, A., Chen, Y., Qyang, Y., Bu, L., Sasaki, M., Martin-Puig, S., et al. (2006). Multipotent embryonic isl1+ progenitor cells lead to cardiac, smooth muscle, and endothelial cell diversification. Cell *127*, 1151–1165.

Naito, A.T., Shiojima, I., Akazawa, H., Hidaka, K., Morisaki, T., Kikuchi, A., and Komuro, I. (2006). Developmental stage-specific biphasic roles of Wnt/beta-catenin signaling in cardiomyogenesis and hematopoiesis. Proc. Natl. Acad. Sci. USA *103*, 19812–19817.

Narazaki, G., Uosaki, H., Teranishi, M., Okita, K., Kim, B., Matsuoka, S., Yamanaka, S., and Yamashita, J.K. (2008). Directed and systematic differentiation of cardiovascular cells from mouse induced pluripotent stem cells. Circulation *118*, 498–506.

Okita, K., Matsumura, Y., Sato, Y., Okada, A., Morizane, A., Okamoto, S., Hong, H., Nakagawa, M., Tanabe, K., Tezuka, K., et al. (2011). A more efficient method to generate integration-free human iPS cells. Nat. Methods *8*, 409–412.

Okita, K., Yamakawa, T., Matsumura, Y., Sato, Y., Amano, N., Watanabe, A., Goshima, N., and Yamanaka, S. (2013). An efficient nonviral method to generate integration-free human-induced pluripotent stem cells from cord blood and peripheral blood cells. Stem Cells *31*, 458–466.

Prall, O.W., Menon, M.K., Solloway, M.J., Watanabe, Y., Zaffran, S., Bajolle, F., Biben, C., McBride, J.J., Robertson, B.R., Chaulet, H., et al. (2007). An Nkx2-5/Bmp2/Smad1 negative feedback loop controls heart progenitor specification and proliferation. Cell *128*, 947–959.

Prasain, N., Lee, M.R., Vemula, S., Meador, J.L., Yoshimoto, M., Ferkowicz, M.J., Fett, A., Gupta, M., Rapp, B.M., Saadatzadeh, M.R., et al. (2014). Differentiation of human pluripotent stem cells to cells similar to cord-blood endothelial colony-forming cells. Nat. Biotechnol. *32*, 1151–1157.

Später, D., Abramczuk, M.K., Buac, K., Zangi, L., Stachel, M.W., Clarke, J., Sahara, M., Ludwig, A., and Chien, K.R. (2013). A HCN4+ cardiomyogenic progenitor derived from the first heart field and human pluripotent stem cells. Nat. Cell Biol. *15*, 1098–1106.

Takahashi, K., Tanabe, K., Ohnuki, M., Narita, M., Ichisaka, T., Tomoda, K., and Yamanaka, S. (2007). Induction of pluripotent stem cells from adult human fibroblasts by defined factors. Cell *131*, 861–872.

Tsai, Y.C., and Weissman, A.M. (2011). Dissecting the diverse functions of the metastasis suppressor CD82/KAI1. FEBS Lett. *585*, 3166–3173.

Uezumi, A., Nakatani, M., Ikemoto-Uezumi, M., Yamamoto, N., Morita, M., Yamaguchi, A., Yamada, H., Kasai, T., Masuda, S., Narita, A., et al. (2016). Cell-surface protein profiling identifies distinctive markers of progenitor cells in human skeletal muscle. Stem Cell Reports *7*, 263–278.

Uosaki, H., Fukushima, H., Takeuchi, A., Matsuoka, S., Nakatsuji, N., Yamanaka, S., and Yamashita, J.K. (2011). Efficient and scalable purification of cardiomyocytes from human embryonic and induced pluripotent stem cells by VCAM1 surface expression. PLoS ONE *6*, e23657.

Woltjen, K., Michael, I.P., Mohseni, P., Desai, R., Mileikovsky, M., Hämäläinen, R., Cowling, R., Wang, W., Liu, P., Gertsenstein, M., et al. (2009). piggyBac transposition reprograms fibroblasts to induced pluripotent stem cells. Nature *458*, 766–770.

Wu, S.M., Fujiwara, Y., Cibulsky, S.M., Clapham, D.E., Lien, C.L., Schultheiss, T.M., and Orkin, S.H. (2006). Developmental origin of a bipotential myocardial and smooth muscle cell precursor in the mammalian heart. Cell *127*, 1137–1150.

Yamashita, J.K. (2016). Expanding reprogramming to cardiovascular progenitors. Cell Stem Cell *18*, 299–301.

Yamashita, J., Itoh, H., Hirashima, M., Ogawa, M., Nishikawa, S., Yurugi, T., Naito, M., Nakao, K., and Nishikawa, S. (2000). Flk1-positive cells derived from embryonic stem cells serve as vascular progenitors. Nature *408*, 92–96.

Yamashita, J.K., Takano, M., Hiraoka-Kanie, M., Shimazu, C., Peishi, Y., Yanagi, K., Nakano, A., Inoue, E., Kita, F., and Nishikawa, S. (2005). Prospective identification of cardiac progenitors by a novel single cell-based cardiomyocyte induction. FASEB J. *19*, 1534–1536.

Yang, L., Soonpaa, M.H., Adler, E.D., Roepke, T.K., Kattman, S.J., Kennedy, M., Henckaerts, E., Bonham, K., Abbott, G.W., Linden, R.M., et al. (2008). Human cardiovascular progenitor cells develop from a KDR+ embryonic-stem-cell-derived population. Nature *453*, 524–528.

Zhang, Y., Cao, N., Huang, Y., Spencer, C.I., Fu, J.D., Yu, C., Liu, K., Nie, B., Xu, T., Li, K., et al. (2016). Expandable cardiovascular progenitor cells reprogrammed from fibroblasts. Cell Stem Cell *18*, 368–381.